COBEM 2023 27TH INTERNATIONAL CONGRESS OF MECHANICAL ENGENEERING

ABCM Brazilian Society of Mechanical Sciences and Engineering
27th ABCM International Congress of Mechanical Engineering
December 04-08, 2023, Florianópolis-SC, Brazil

COB-2023-0849
NUMERICAL SIMULATION OF A GAS PLAIN SEAL FOR ROTORDYNAMIC COEFFICIENTS CALCULATIONS USING OPEN-SOURCE SOFTWARE

Franco Barbi
João Marcelo Vedovotto
Aldemir Aparecido Cavallini Junior
Aristeu da Silveira Neto
Universidade Federal de Uberlândia - Av. João Naves de Ávila, 2121, Uberlândia - MG
frcbarbi@gmail.com; vedovotto@ufu.br; aacjunior@ufu.br; aristeus@ufu.br

Raphael Timbó Silva
CENPES/PETROBRAS - Av. Horácio Macedo, 950, Rio de Janeiro - RJ
raphaelts@petrobras.com.br

Abstract. *Gas seals are used in compressors and turbines to suppress fluid leakage while enabling shaft rotation through multiple regions at different pressure levels. There are many types of seals: plain, labyrinth, hole pattern, honeycomb; each one with its performance and geometric characteristics. Turbomachinery in the Gas & Oil industry operates at severe conditions due to productivity requirements. In many cases, elevated rotation frequencies are desired but often limited by equipment's vibrational stability. Therefore, it is crucial to understand the rotordynamic behavior of these machines and how each component affects the system in order to enhance design quality and optimize maintenance activity. During operation of seals, fluid dynamic forces interacting with rotor's and stator's surfaces contribute to rotordynamic coefficients and its evaluation based on modeling is of great interest. Models based on the bulk-flow theory have the advantage of low processing costs but its simplification hypothesis can be limiting, especially for seals with complex geometry. Such models can be improved with results obtained from models that solve the complete set of constitutive equations for fluid flows, i. e., mass conservation, Newton's Second Law of motion and energy conservation. Despite the elevated computational capacity required, the rapid advance of hardware technology and numerical methods is enabling the usage of Computational Fluid Dynamics (CFD) to investigate the phenomena present in seal's flows and improve rotordynamic coefficient calculations. The aim of this research work is to evaluate the application of the open-source CFD library OpenFOAM base solvers in the calculation of rotordynamic coefficients in plain seals with compressible flows. Results are explored for different rotational shaft velocity and different outlet total pressure. Comparisons with literature data obtained from experiments, with CFD/open-source, CFD/commercial, bulk-flow based models are also presented, contributing with the discussion of the advantages and drawbacks when using the method.*

Keywords: *Plain seal, OpenFOAM, rotordynamic coefficients*

1. INTRODUCTION

Annular seals used in rotary machines are crucial to the well functioning of the system and its design should meet stability requirements for a given operational condition. The component is responsible to minimize fluid leakage through different chambers at different pressure levels and directly affects system's efficiency. Furthermore, forces generated during its operation contributes to the dynamic behavior of the rotating machines. To improve the design of seals, it is very useful to be able to predict leakage and forces acting on seals through modelling. The most used models to predict leakage and rotordynamic coefficients are based on Reynolds equations and the bulk-flow theory (Hirs, 1973). Both are simplified forms of the three-dimensional Navier-Stokes equations, based on thin films characteristics. Therefore, the accuracy of rotordynamic coefficients obtained with these models may be questionable, mainly when seal's geometry is different from that which was considered in the development of the model. Experimental comparisons have exposed such differences and, despite its important contribution to validations, information is limited by the number of sensors and its intrusive characteristic. With recent computational technology advances and availability, an interesting alternative is the usage of three-dimensional models based on the complete Navier-Stokes equations, as it is performed in the Computational Fluid Dynamics field. Besides obtaining coefficients directly, CFD models can be used to improve simplified models, such as those derived from Reynolds equations and bulk-flow theory.

In the context of three-dimensional CFD simulations, rotordynamic coefficients of annular seals have been obtained through three different methods (Snyder and Santos, 2021):

- Perturbed equations: small, harmonic perturbations of the flow variables are introduced into the Navier-Stokes and turbulence transport equations (Dietzen and Nordmann, 1987). Equations are expanded with Taylor series and, when solved, enables the construction of stationary properties fields and seal's rotordynamic forces/coefficients;
- Whirling Rotor Method: analysis considering a whirling movement of the rotor around the center of the seal. Navier-Stokes and transport equations are solved in a reference frame system at the seal's center that rotates at whirling velocity (Tam *et al.*, 1987; Athavale *et al.*, 1995). For constant whirling velocities, stationary solutions can be obtained without the need of mesh movement and computational expensive transient solutions;
- Numerical shaker (Przekwas and Athavale, 1992): is the analog of experimental shaker modal analysis methods. Consists in solving the complete set of Navier-Stokes equations, modeling rotor's movement through mesh deformation. Despite being the most time consuming method, it is the most flexible one, allowing non-circular movements and analysis of relatively big rotor amplitudes. Resulting forces can be used to calculate rotordynamic coefficients through curve fitting, or build a frequency response function for the calculation of rotordynamic seal forces.

The research published by Tam *et al.* (1987) presented a three-dimensional Navier-Stokes model to investigate rotor's instabilities and its causing factors. Using a relative reference frame rotating with the same whirling velocity of the rotor, authors showed that the entrance pre-swirl of the fluid flow, when rotating in the opposite direction from the rotating journal, causes a reduction on the mean circumferential velocity through the increase of recirculation zones. Years later, Athavale *et al.* (1995) applied the same method to validate the complex flow generated by the whirling motion and validated with experimental results. Other researches algo applied the Whirling Rotor Method (Moore, 2003; Tsukuda *et al.*, 2017; Ha and Choe, 2012; Untaroiu *et al.*, 2012; Kim and Ha, 2016).

Numerical simulations of a compressible flow through a plain annular seal for rotordynamic coefficients calculations were performed by Ha and Choe (2014), also using the Whirling Rotor Method. Besides these results, authors also presented others obtained from a bulk-flow based model. For the CFD simulation, Ansys® Fluent software was used to model the turbulent compressible flow, with ideal gas model and $\kappa - \epsilon$ turbulence model. Their results were compared against experimental data from Dunn (1990), registering an over-prediction of the leakage by 35.8% when compared with experimental values. In addition, the authors observed an improvement of rotordynamic coefficients when compared with values obtained by the bulk-flow based model.

Snyder and Santos (2021) also presented numerical results of CFD simulations with the Whirling Rotor Method, comparing with data from literature for compressible and incompressible flows through annular plain seals. The authors used the open-source library OpenFOAM and registered unsatisfactory results for the compressible flow cases. Then, for compressible flows, results were also obtained with Ansys® Fluent software, where good comparisons with literature were registered.

The present work presents results of calculations of rotordynamic coefficients obtained with the Whirling Rotor Method using the open-source library OpenFOAM, for the compressible flow through the same annular seal first presented experimentally by Dunn (1990) and later used for numerical validations of Ha and Choe (2014) and Snyder and Santos (2021).

2. NUMERICAL MODEL

Numerical simulations for the analysis of leakage and rotordynamic forces/coefficients were performed with a base solver (rhoPimpleFoam) built with open-source library OpenFOAM-9, distributed by Openfoam Foundation. Governing equations are discretized with Finite Volume Method with a co-located arrangement of variables. The SIMPLE (Semi-Implicit Method for Pressure Linked Equations) algorithm is used to solve the Navier-Stokes equations with pressure-velocity coupling. Several turbulence models are also available for selection with basic wall functions for boundary treatment. In the current research, the $\kappa\omega - SST$ as presented by Menter and Esch (2001) is applied for turbulence modeling. To represent a whirling rotor, the used solver relies on a Multiple Reference Formulation, which allows users to define relative observers rotating with a given velocity, designed for rotary machines applications.

2.1 Mathematical Formulation

The governing equations for the compressible flow is modeled with mass conservation equation (Eq. 1), Navier-Stokes equations (2), energy equation (3) and a equation of state, in the current case, an ideal gas equation (4). The superscript ($\bar{}$) refers to filtered quantities that are produced by RANS turbulence modeling.

$$\frac{\partial \bar{\rho}}{\partial t} + \nabla \cdot (\bar{\rho}\bar{u}) = 0. \tag{1}$$

$$\frac{\partial \bar{\rho}\bar{u}}{\partial t} + \nabla \cdot (\bar{\rho}\bar{u}\bar{u}) = -\nabla \bar{p} + \nabla \cdot \bar{\tau} + \bar{\rho} g. \tag{2}$$

$$\frac{\partial(\bar{\rho}\bar{e})}{\partial t} + \nabla \cdot (\bar{\rho}\bar{u}\bar{e}) = \nabla \cdot \left[k_{eff}\nabla\bar{T} - \bar{p}\bar{u}\right]. \tag{3}$$

$$\bar{\rho} = \sqrt{\frac{\bar{p}}{R\bar{T}}}. \tag{4}$$

2.2 MRF - Multiple Reference Frame

To define a new reference frame to solve Navier-Stokes equations, used must provide its center position and a rotating velocity Ω. Equations modeled by the MRF approach also solves for the absolute velocity u, although transport fluxes are calculated with a relative velocity u_r, as presented in Eq. 5. Then, Navier-Stokes equations is modified as presented by Eq. 6, in which an additional term is considered in the formulation. Since it still solves for the absolute velocity, no further modifications are necessary in Eqs. 1 and 3.

$$\bar{u_r} = \bar{u} - (\Omega \times r). \tag{5}$$

$$\frac{\partial\bar{\rho}\bar{u}}{\partial t} + \nabla \cdot (\bar{\rho}\bar{u_r}\bar{u}) + \rho(\Omega \times \bar{u}) = -\nabla\bar{p} + \nabla \cdot \bar{\tau} + \bar{\rho}g. \tag{6}$$

2.3 Whirling Rotor Method

The Whirling Rotor Method enables the calculation of rotordynamic coefficients with steady state solutions of a rotating reference frame that models a whirling movement of a rotor around a seal's center. The movement acts as a perturbation of the dynamic system and, with proper simplifications, the coefficients can be obtained through curve fitting of resulting forces. Figure 1 presents a schematic of the seal and the rotating reference frame.

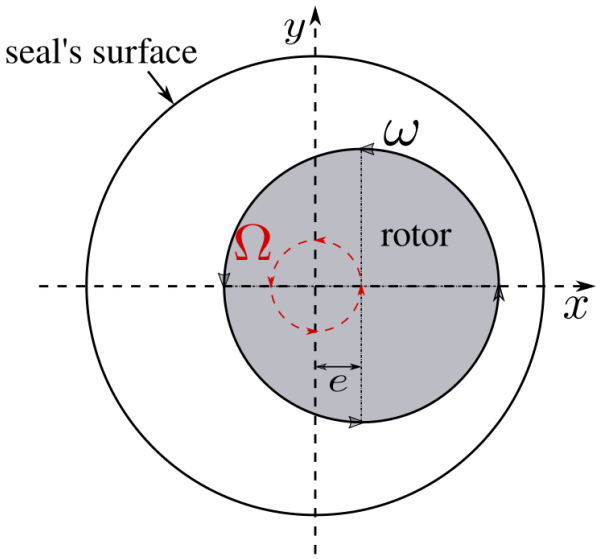

Figure 1. Schematic figure of the seal and rotor section with a rotating reference frame.

The dynamic system composed by a seal and a rotor can be expressed by Eq. 7.

$$\begin{Bmatrix} -F_x(t) \\ -F_y(t) \end{Bmatrix} = \begin{bmatrix} K_{xx} & K_{xy} \\ K_{yx} & K_{yy} \end{bmatrix} \begin{Bmatrix} x \\ y \end{Bmatrix} + \begin{bmatrix} C_{xx} & C_{xy} \\ C_{yx} & C_{yy} \end{bmatrix} \begin{Bmatrix} \dot{x} \\ \dot{y} \end{Bmatrix} + \begin{bmatrix} M_{xx} & M_{xy} \\ M_{yx} & M_{yy} \end{bmatrix} \begin{Bmatrix} \ddot{x} \\ \ddot{y} \end{Bmatrix}. \tag{7}$$

In the present work, the same simplifications adopted by Ha and Choe (2014) are used: virtual mass terms are neglected, and $K_{xx} = K_{yy}$, $K_{xy} = -K_{yx} = k$, $C_{xx} = C_{yy}$, $C_{xy} = -C_{yx} = c$. Thus, the dynamic system can be represented by Eq. 8. The whirling movement translates the center of the rotor at a distance e from the center of the seal. Considering a perturbation in the form of Eq. 9, one can write expressions as presented by Eq. 10. Once obtained the forces acting on the rotor for different whirl velocities Ω, rotordynamic coefficients are obtained with curve fitting.

$$\begin{Bmatrix} -F_x(t) \\ -F_y(t) \end{Bmatrix} = \begin{bmatrix} K & k \\ -k & K \end{bmatrix} \begin{Bmatrix} x \\ y \end{Bmatrix} + \begin{bmatrix} C & c \\ -c & C \end{bmatrix} \begin{Bmatrix} \dot{x} \\ \dot{y} \end{Bmatrix}. \tag{8}$$

$$\begin{cases} x = e \cdot \cos(\Omega t) \\ y = e \cdot \sin(\Omega t) \end{cases} \tag{9}$$

$$\begin{cases} \dfrac{F_x}{e} = -K - c\Omega \\ \dfrac{F_y}{e} = k - C\Omega \end{cases} \tag{10}$$

2.4 Computational Domain and Boundary Conditions

Computational mesh is constructed with the blockMesh application, from OpenFOAM. Hexahedral cells are distributed along the domain, as illustrated in Fig. 2. For near wall treatment, mesh stretching is used to ensure suitable refinement. Rotor's eccentricity relative to the seal's center is set shifting the rotor's center position in the direction of positive x, as indicated in Fig. 1. For the present work, 35 cells across radial clearance was used, while cell number in circumferential (θ) and axial directions (z) were determined to maintain the relation $^{\Delta\theta}/_{\Delta z} \approx 1$.

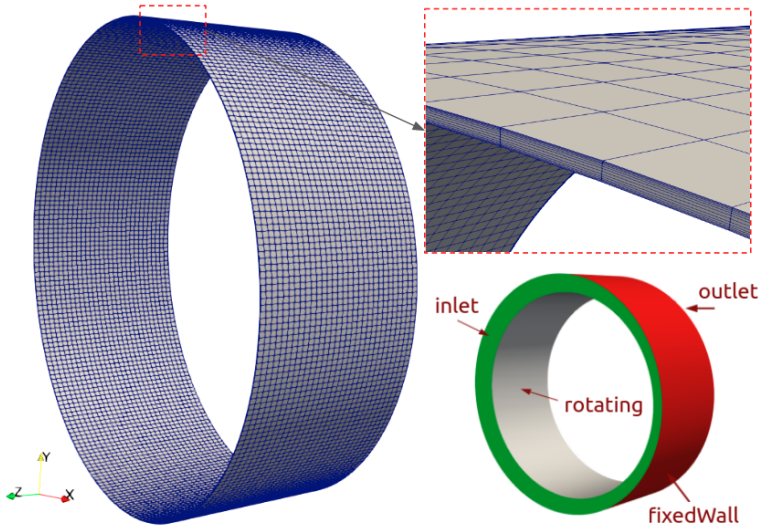

Figure 2. Schematic figure of the seal and rotor section with a rotating reference frame.

Table 1 presents the dimensions and operation conditions of a plain seal first presented by Dunn (1990), which rotordynamic coefficients obtained were later compared with numerical results of Ha and Choe (2014) and Snyder and Santos (2021). In this work, eccentricity was considered 1% of the radial clearance, as indicated in the table.

Boundary conditions are set with the prescription of the total pressure in the inlet and outlet of the seal. For the velocity, a mixed type condition is used to impose a pre-swirl condition for the radial and circumferential directions, while a homogeneous Neumann condition is used for the axial velocity. With this conditions, the leakage flow is promoted by the pressure difference in the inlet and outlet faces. The pre-swirl is defined as tha ratio between entrance fluid rotation velocity and shaft rotation velocity. For this research, pre-swirl is set to zero as in the work of Snyder and Santos (2021), since the pre-swirl was not directly provided in the experimental description of Dunn (1990) (Snyder and Santos, 2021). For the seal's surface (fixedWall in Fig. 2), a no slip condition is imposed, while at rotor's surface (rotating in Fig. 2) a tangential velocity is used to model shaft's rotation.

3. RESULTS

Simulation results are presented in three parts. First, a mesh test is presented comparing rotordynamic coefficients and flow leakage with literature data. A percentage of value deviation is presented in relation to experimental data of Dunn (1990), as expressed by Eq. 11.

Table 1. Dimensions and operation conditions of the plain seal first presented by Dunn (1990).

Seal's radius (R)	76.2 [$\times 10^{-3}$ m]
Seal's lenght (L)	50.8 [$\times 10^{-3}$ m]
Radial clearance (C)	0.2286 [$\times 10^{-3}$ m]
Excentricity (e)	1% of radial clearance
Inlet total pressure (P_{in})	7.86 [$\times 10^{5}$ Pa]
Outlet total pressure (P_{out})	4.339; 3.836; 3.2; 2.657 [$\times 10^{5}$ Pa]
Rotational shaft speed (ω)	526.74; 1256.64; 1675.52 [rad/s]
Viscosity (μ)	1.9 [$\times 10^{-5}$N $\cdot$ s/m^2]
Gás constant (R)	287 [J/Kg $\cdot$ K]
Gamma (γ)	1.4

$$\epsilon = 100\frac{(\phi_s - \phi_{exp})}{\phi_{exp}} \ [\%]. \tag{11}$$

In the second part, direct stiffness and cross-coupled stiffness are calculated for different rotational shaft speeds, and results are compared to the data of Dunn (1990) and Ha and Choe (2014). The third part of results compares the coefficients obtained for different outlet pressure values. For curve fitting, results were generated for six different whirling velocities expressed by fractions of shaft velocity: 0, 0.2, 0.4, 0.6, 0.8 and 1. Figure 3 presents the values of F_x/e and F_y/e obtained for different whirling velocities fractions.

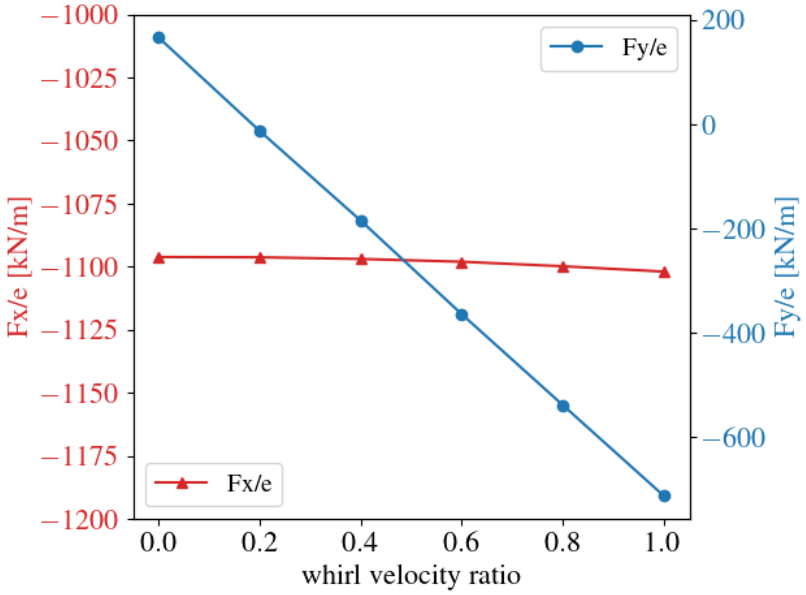

Figure 3. Schematic figure of the seal and rotor section with a rotating reference frame.

3.1 Mesh test

Cells dispositions of used meshes are showed in Tab. 2. Each of them have 35 cells in the radial direction (radial clearance) with mesh stretching towards stator's and rotor's walls, resulting in Y+ values in the range of 2.2 < Y+ < 2.9. Table 3 shows comparisons of rotordynamic coefficients obtained with literature data. One can notice that, in general, current results agrees well with experimental results of Dunn (1990). Direct stiffness coefficients obtained with present model deviates to values lower than experimental, with a maximum deviation of -14.9% for the coarsest mesh and -9.75% for the finest. Major deviations are observed for the cross-coupled stiffness, with overpredictions of experimental values above 35%, with a maximum of 48.08% in the finest mesh result. Other results from literature significantly underpredicted the cross-couple stiffness coefficients. These deviations from experimental data might be explained for the lack of details regarding the fluid pre-swirl at seal's inlet. For the direct damping coefficients, present results agree very well with experimental data, while other simulation references registered considerably higher values of deviation. One can notice

Table 2. Cell disposition of meshes used in mesh test.

	n_θ	n_z	n_r	Total cells
Mesh 1	188	30	35	131600
Mesh 2	282	40	35	296100
Mesh 3	376	60	35	526400
Mesh 4	565	80	35	1186500
Mesh 5	753	80	35	2108400

Table 3. Rotordynamic coefficients obtained in mesh test and comparisons with literature data.

	$K_{xx} = K_{yy}$		$K_{xy} = -K_{yx}$		$C_{xx} = C_{yy}$		Leakage	
	[kN/m]	ϵ [%]	[kN/m]	ϵ [%]	[kNs/m]	ϵ [%]	[kg/s]	ϵ [%]
Dunn (1990) Experimental	1241.83	-	117.17	-	1.63	-	0.076	-
Ha and Choe (2014) Fluent	1061.55	-14.52	61.25	-47,73	1.46	-10,43	0.104	36,84
Snyder and Santos (2021) Fluent	1334.92	7.50	40.41	-65,51	2.00	22,70	0.107	40,79
Snyder and Santos (2021) OpenFoam	1012.20	-18.49	55.93	-52,27	0.21	-87,12	0.106	39,47
Mesh 1	1056.74	-14.9	161.59	37.91	1.59	-2.45	0.0830	9.3
Mesh 2	1083.96	-12.71	159.12	35.8	1.63	0.0	0.0828	9.0
Mesh 3	1096.18	-11.73	165.24	41.03	1.67	2.45	0.0827	8.88
Mesh 4	1100.66	-11.37	162.58	38.76	1.69	3.68	0.0826	8.8
Mesh 5	1120.72	-9.75	173.51	48.08	1.71	4.91	0.0826	8.77

an expressive underprediction of OpenFoam result in the work of Snyder and Santos (2021), where authors affirmed that their OpenFoam model was unable to capture the effects of the whirling motion for compressible flows in plain seals. Mass leakage calculations throughout the seals were also compared, and present results are closer to experimental measurements than all other references presented (> 35%), with deviations values under 10% from experimental value.

The results presented on Tab. 3 showed that current model is able to predict rotordynamic coefficients in reasonable agreement with literature data, despite the significant deviations of the cross-coupled stiffness. Mesh refinement in the circumferential and axial directions led to lower deviations from experimental data for all parameters but cross-coupled stiffness coefficients. The matter should be addressed in future investigations. For comparisons of coefficients at different operation conditions, Mesh 3 configuration was used and results are showed in next sections.

3.2 Stiffness Coefficients Variations with Shaft Rotation Velocity

Figure 4 presents direct stiffness coefficients K and cross-coupled stiffness coefficients k obtained with present model. Results are compared with results from CFD and bulk-flow based model (BFM) of Ha and Choe (2014), and experimental results of Dunn (1990).

For the direct stiffness, results from current model is closer to experimental for $\omega = 526.74$ rad/s when compared with literature data. For shafts velocities of 1256.64 rad/s and 1675.52 rad/s, the model presented underpredicted experimental values approximately by 30 % and 50 %, respectively. Also, coefficients obtained in results decreased in a straight line as shaft speed augmented. Among literature results presented, only the BFM of Ha and Choe (2014) showed a similar behavior, while other data suggested a slight increase in direct stiffness when changing from 1256.64 rad/s to 1675.52 rad/s.

In the case of cross-coupled stiffness, present results overpredicted by 41.03 % experimental values for shaft rotational speed of 526.74 rad/s, while Ha and Choe (2014) CFD model underpredicted in 47.73 %, while the bulk-flow based model from the same authors underpredicted by 64 %. For shaft rotational velocity of 1256.64 rad/s, the result value surpass experimental data in 28.17 % , while Ha and Choe (2014) models showed values 41% lower for the CFD model and 48% for the bulk-flow based model. For the shaft velocity of 1675.52 rad/s, results was 7.7 % lower than experimental, while results from Ha and Choe (2014) was approximately 40 % lower.

3.3 Stiffness, damping and leakage variations with outlet pressure

Figure 5-8 shows resulting coefficients varying with outlet total pressure P_{out}, for a rotational shaft velocity of 526.74 rad/s, and comparisons with data from Dunn (1990), Ha and Choe (2014) and Snyder and Santos (2021). In Fig. 5, one can observe values of direct stiffness with similar behavior when outlet pressure varies. Despite deviations of values among data, its possible to notice that results obtained with Fluent presented points almost forming a line segment, different from all other results. For increasing values of outlet pressure presented in Tab. 1, present results are below experimental values

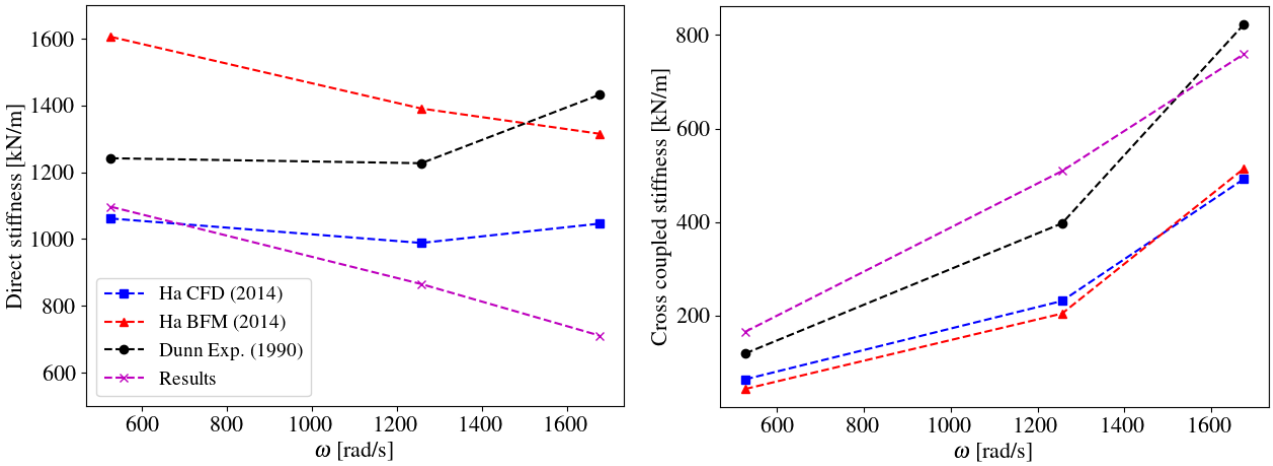

Figure 4. Direct and cross-coupled stiffness variations with rotational shaft velocity ω and comparisons with literature data.

of Dunn (1990) by 73.9%, 4.5%, 14.3% and 11.8%, respectively. Major deviances of current results are observed in Fig 6 for cross-coupled stiffness, with overpredictions of 105.28%, 118.31%, 74.05% and 41.03% for the increasing pressure values, respectively. All other results presented values about 23% to 30% lower than experimental results. This evident deviation may be explained by different wall treatments, possibly different pressure boundary conditions and the lack of details about the flow's pre-swirl at the seal's inlet, as indicated in the work of Snyder and Santos (2021).

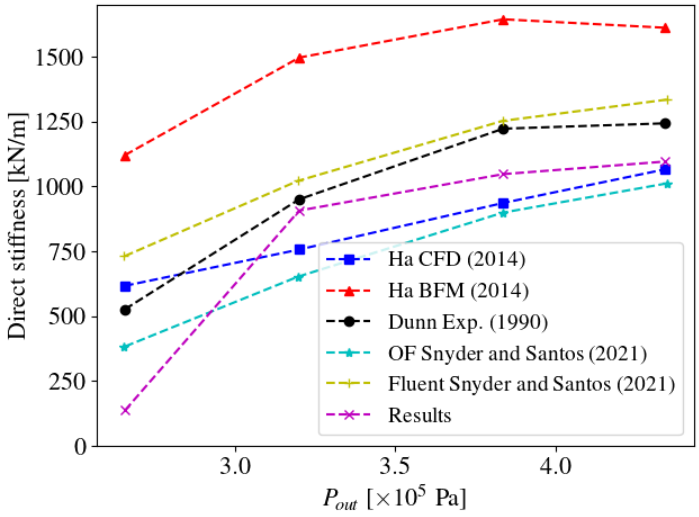

Figure 5. Direct stiffness variations with outlet total pressure P_{out} and comparisons with literature data.

In the case of direct damping coefficients, as showed in Fig. 7, the current model presented values in very good agreement with experimental data, with deviations (Eq. 11) of -14.61 %, -7.19 %, -0.83 % and 2.27 %, for the increase of outlet pressure presented in Tab. 1, respectively. Its noticeable that results from OpenFOAM obtained by Snyder and Santos (2021) substantially deviates from all compared data. Authors claims that their model was not able to execute the Whirling Rotor Method accurately, and this motivated the usage of Fluent for calculation of rotordynamic coefficients of tha plain seal with compressible flow.

Figure 8 presents a comparison of leakage flow through the plain seal for a zero whirling velocity, where its possible to observe how well the present model was able to predict the mass flow rate obtained by experiments of Dunn (1990), in comparison to values obtained by Ha and Choe (2014) and Snyder and Santos (2021). For the increasing values of pressure, leakage results are exceeding experimental ones by 10.17 %, 9.79 %, 8.68 % and 8.88%.

4. CONCLUSIONS

The present research modeled a compressible flow through an annular plain seal with the rhoPimpleFoam solver from OpenFOAM-9, using the Whirling Rotor Method to calculate rotordynamic coefficients with different rotational shaft

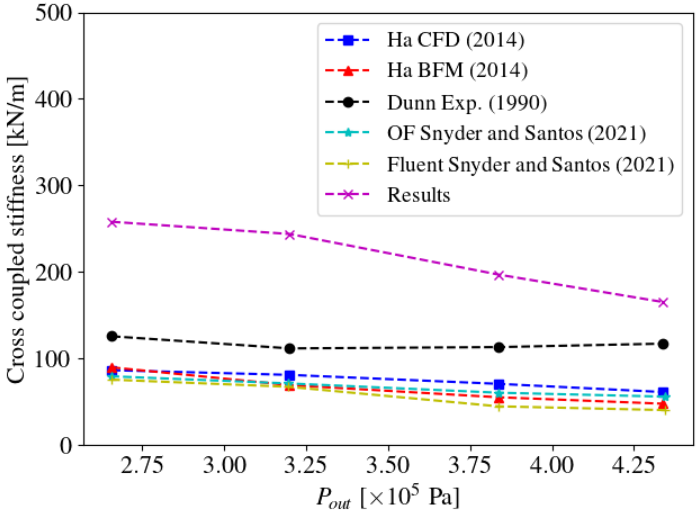

Figure 6. cross-coupled stiffness variations with outlet total pressure P_{out} and comparisons with literature data.

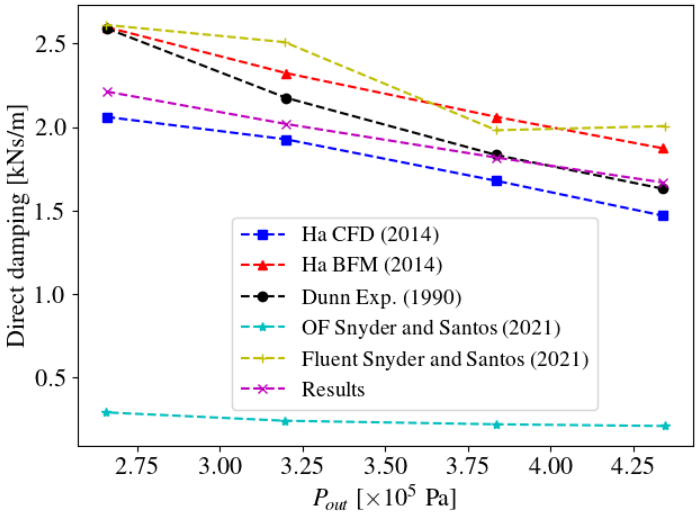

Figure 7. Direct damping variations with outlet total pressure P_{out} and comparisons with literature data.

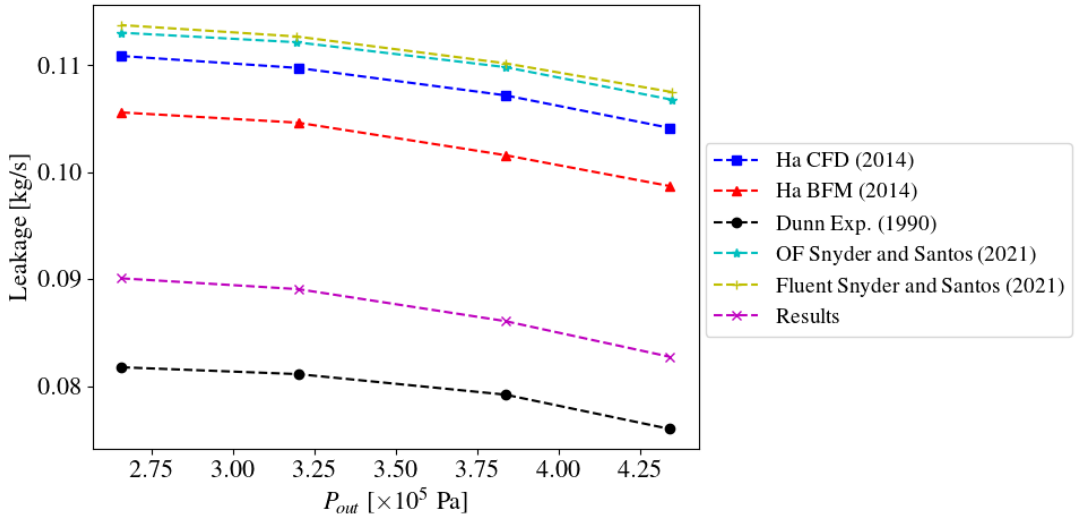

Figure 8. Variations of leakage through the seal with outlet total pressure P_{out} and comparisons with literature data.

velocity and outlet total pressure. Results were compared with experimental results from Dunn (1990) and numerical results from Ha and Choe (2014) and Snyder and Santos (2021). Comparisons showed that the present model is able to predict rotordynamic coefficients with relative accuracy. It is important to highlight that while current results for cross-coupled stiffness significantly overpredicted values from references, present leakage results were closer to experimental values when compared to other models from literature.

5. ACKNOWLEDGEMENTS

The authors would like to thank CNPq, FAPEMIG and CAPES (INCT-EIE) for the financial support of this contribution. The authors also thank Petrobras for the technical and financial support, through the Research and Development project PT-200.20.00169 – "Artificial intelligence applied in the creation of representative models of hydrodynamic bearings, annular seals and rotating machines (ROSS-Digital Twin) " with technical management of CENPES/PDIDP/ESUP/TIS.

6. REFERENCES

Athavale, M., Hendricks, R.C. and Steinetz, B.M., 1995. "Numerical simulation of flow in a whirling annular seal and comparison with experiments". Technical report.

Dietzen, F. and Nordmann, R., 1987. "Calculating rotordynamic coefficients of seals by finite-difference techniques".

Dunn, M.S., 1990. "Comparison of experimental results and theoretical predictions for the rotordynamic coefficients of stepped annular gas seals". *P.H.D. Thesis*.

Ha, T.W. and Choe, B.S., 2012. "Numerical simulation of rotordynamic coefficients for eccentric annular-type-plain-pump seal using cfd analysis". *Journal of mechanical science and technology*, Vol. 26, pp. 1043–1048.

Ha, T.W. and Choe, B.S., 2014. "Numerical prediction of rotordynamic coefficients for an annular-type plain-gas seal using 3d cfd analysis". *Journal of mechanical science and technology*, Vol. 28, pp. 505–511.

Hirs, G.G., 1973. "A Bulk-Flow Theory for Turbulence in Lubricant Films". *Journal of Lubrication Technology*, Vol. 95, No. 2, pp. 137–145. ISSN 0022-2305. doi:10.1115/1.3451752. URL `https://doi.org/10.1115/1.3451752`.

Kim, S.H. and Ha, T.W., 2016. "Prediction of leakage and rotordynamic coefficients for the circumferential-groove-pump seal using cfd analysis". *Journal of Mechanical Science and Technology*, Vol. 30, pp. 2037–2043.

Menter, F. and Esch, T., 2001. *16th Brazilian Congress of Mechanical Engineering - COBEM*, Vol. 134, No. 2.

Moore, J.J., 2003. "Three-dimensional cfd rotordynamic analysis of gas labyrinth seals". *Journal of Vibration and Acoustics*, Vol. 125, No. 4, pp. 427–433. ISSN 1048-9002. doi:10.1115/1.1615248. URL `https://doi.org/10.1115/1.1615248`.

Przekwas, A. and Athavale, M., 1992. "Development of a cfd code for fluid dynamic forces in seals". In *Proceedings of the 1992 seals flow development workshop (CP-10124). NASA Lewis Research Center, Cleveland*. pp. 68–84.

Snyder, T. and Santos, I., 2021. "Rotordynamic force estimation of turbulent, annular seals using openfoam®". *Journal of the Brazilian Society of Mechanical Sciences and Engineering*, Vol. 43, No. 3, p. 119.

Tam, L., Przekwas, A., Muszynska, A., Hendricks, R., Braun, M. and Mullen, R., 1987. "Numerical and analytical study of fluid dynamic forces in seals and bearings". Technical report.

Tsukuda, T., Hirano, T., Watson, C., Morgan, N.R., Weaver, B.K. and Wood, H.G., 2017. "A numerical investigation of the effect of inlet preswirl ratio on rotordynamic characteristics of labyrinth seal". Vol. Volume 7A: Structures and Dynamics of *Turbo Expo: Power for Land, Sea, and Air*. doi:10.1115/GT2017-64745. URL `https://doi.org/10.1115/GT2017-64745`. V07AT34A029.

Untaroiu, A., Untaroiu, C.D., Wood, H.G. and Allaire, P.E., 2012. "Numerical modeling of fluid-induced rotordynamic forces in seals with large aspect ratios". *Journal of Engineering for Gas Turbines and Power*, Vol. 135, No. 1. ISSN 0742-4795. doi:10.1115/1.4007341. URL `https://doi.org/10.1115/1.4007341`. 012501.

7. RESPONSIBILITY NOTICE

The following text, properly adapted to the number of authors, must be included in the last section of the paper:
The author(s) is (are) solely responsible for the printed material included in this paper.